 CMES, vol.18, no.2, pp.145-153, 2007

Structural Arrangement Effects of Mineral Platelets on the Nature of Stress Distribution in Bio-Composites

S. Anup [1], S. M. Sivakumar[2] and G. K. Suraishkumar[3]

Abstract: Bone is a hierarchical bio-composite, and has a staggered arrangement of soft protein molecules interspaced with hard mineral platelets at the fine ultrastructure level. The investigation into reasons for high fracture toughness of bio-composites such as bone requires consideration of properties at the different levels of hierarchy. In this work, the analysis is done at the continuum level, but the properties used are appropriate to that of the level considered. In this way, the properties at the fine ultrastructure level of bone is considered in the stress distribution analysis of a platelet adjacent to the broken platelet. Results show the influence of overlapping in determining the nature of stress distribution. This could play an important part in the fracture toughness of bio-composites.

Keyword: Bone, Bio-composites, Fracture toughness, Overlapping, Shear lag

1 Introduction

Bone, Nacre and Dentin are some examples of natural composites that achieve their high fracture toughness due to their hierarchical structure (Menig, Meyers, Meyers, and Vecchio, 2000). Bone has got a hierarchical structure, with about seven levels of hierarchy (Rho, Kuhn-Spearing, and Zioupos, 1998). It is a composite of protein (collagen) and mineral. At the fine ultrastructure level, bone is composed of mineralized collagen fibrils made up of collagen molecules interspaced with mineral crystals.

[1] Department of Applied Mechanics, Indian Institute of Technology Madras, Chennai-600036, India.
[2] Department of Applied Mechanics, Indian Institute of Technology Madras, Chennai-600036, India.
[3] Department of Biotechnology, Indian Institute of Technology Madras, Chennai-600036, India.

It has been observed that the collagen molecules have a staggered arrangement and the minerals occupying the gaps between the collagen molecules also have a staggered or overlapping arrangement (Fratzl, Gupta, Paschalis, and Roschger, 2004). An idealised arrangement would consist of staggered mineral platelets in a collagen matrix as shown in Fig. 1. This type of idealised models were used by other researchers also, which were supported by the above mentioned experimental observations (Fratzl, Gupta, Paschalis, and Roschger, 2004; Ji and Gao, 2004).

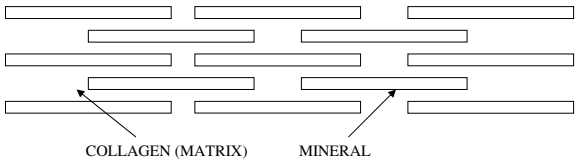

Figure 1: Idealised Arrangements of Mineral Platelets

The study of bone fracture is important from a clinical point of view. Many studies have been conducted on modeling of bone and bone fracture (Muller-Karger, Gonzalez, Aliabadi, and Cerrolaza, 2001; Ji and Gao, 2004). The influence of structural arrangement on stress distribution in a platelet adjacent to a broken platelet is the focus of this paper since this can have an effect on the fracture toughness of bone. It has been shown by Vashishth, Behiri, and Bonfield (1997) that when a crack propagates in bone, microcracks are produced ahead of the crack tip as well as in the crack wake. These microcracks are believed to be beneficial in dissipating the energy available at the crack tip, there by toughening the material.

Another school of thought believes that they also weaken the material under certain conditions, especially, when there are increased levels of microcracking (Nalla, Kruzic, and Ritchie, 2004; Yeni and Fyhrie, 2002). Also, other researchers have observed that bone samples from older humans show an increase in microcracking (Schaffler, Choi, and Milgrom, 1995). This results in a decrease in the initiation and propagation fracture toughness (Nalla, Kruzic, Kinney, Balooch, Ager III, and Ritchie, 2006) in such samples. This implies that microcracks may reduce the ability of bone to resist fracture. On the other hand, Wang and Qian (2006) argue that if the cracks are formed as diffuse damage, it is beneficial from a fracture mechanics point of view since it will dissipate more energy than microcracks. This will starve the crack tip of energy available for macrocrack propagation. Also, diffuse damage may be the preferred option of energy dissipation given the detrimental nature of microcracks.

The fracture toughness of bio-composites is influenced by the macroscopic constitutive response of the constituent materials. For example, the viscoelasticity of protein can dissipate large amount of fracture energy thereby making the bio-composites tougher (Ji and Gao, 2004). The high fracture toughness of nacre is also attributed to the modular damage evolution of the organic matrix (Nukala and Simunovic, 2005). The nature of stress distribution in a platelet adjacent to the broken platelet, may also play a role in the nature of cracks that are formed (microcracks or diffuse damage) as given in Fig. 2, following the work of Wang and Qian (2006). This also may be expected to influence the fracture toughness of bone.

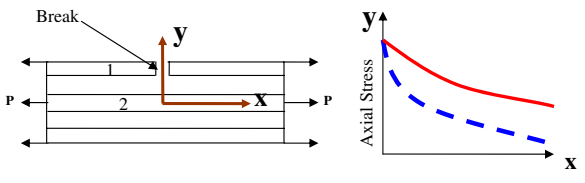

Figure 2: (a) Simplified model of fine ultrastructure of bone and (b) Nature of Stress distribution

The way in which bio-composites like bone resist fracture, specifically the contribution of the fine ultrastructure had been looked into by many researchers (Ji and Gao, 2004; Wang and Qian, 2006) employing various methodologies. One of the methods used was the virtual internal bond method (VIB) (Ji and Gao, 2004; Zhang, Klein, Huang, Gao, and Wu, 2002). Though Ji and Gao (2004), have considered a staggered arrangement as seen in experimental observations, they assume that the platelets are intact. In a diffuse damage situation, the fracture toughness may be related to the post-breakage of platelets. Wang and Qian (2006) and Kotha, Kotha, and Guzelsu (2000) have shown that a simple shear lag theory is a good candidate for analysis of the stress distribution and fracture at the nanolevel.

The stress distribution in a fiber adjacent to a broken fiber was investigated by many researchers using shear lag theory (Hedgepeth, 1961; Goree and Gross, 1980). Wang and Qian (2006) extended this idea for the case of mineral platelets in bone. They used a simplified model of aligned mineral platelets and found the effect of stress distribution in mineral platelets on the fracture toughness of bone. The stress distribution in overlapping mineral platelets were found by Kotha, Kotha, and Guzelsu (2000). Also, Ji and Gao (2004) concluded that the staggered or overlapping arrangement and high aspect ratio of mineral platelets are the reasons for the high modulus of bio-composites. These studies point to the importance of overlapping arrangement of mineral platelets in providing bone with desired properties. Therefore, a better and critical structural model for assessing fracture toughness would be to consider the stress distribution on an adjacent platelet on account of breakage in a platelet within an overlapped arrangement. This study is expected to provide more insight into the fracture process in bone.

In the present work, the objective of the analysis is thus, aimed at finding out the effect of overlapping on stress distribution on a platelet adjacent to the broken platelet in a bio-composite.

2 Formulation of the problem

A simple idealised model is employed in which structural arrangement of overlapping platelets of mineral is bound together by collagen molecules, since this model retains the physical features of the bone at the nanoscale, like the overlapping arrangement of mineral platelets. Also, this model is easily amenable to analysis. In this work shear lag theory is used for analysis. The method being simple and computationally inexpensive renders the advantages necessary for a parametric study that is cost effective and at the same time reasonably accurate. Shear-lag analysis has been shown to be accurate, when compared with FE analysis (Reedy, 1984). FE analysis for certain cases is done for comparison. In this work, we assume that the mineral platelets are perfectly bonded to the matrix. It is assumed that the only failure mode is by breakage of mineral platelets, since this is a significant way of failure of mineral platelets as shown by experiments (Sahar, Hong, and Kohn, 2005). The load applied is assumed to act along the direction of alignment of mineral platelets, due to the fact that this could be critical. The region around broken fibers show a rise in stress (Hedgepeth, 1961), causing failure in adjacent platelets. Hence, the objective is to find out the stress distribution in a platelet adjacent to a broken platelet.

2.1 Shear Lag Model

The formulation of the shear lag model used in this work is similar to that has been reported earlier (Kotha, Kotha, and Guzelsu, 2000). The idealised unit cell model used is shown in Fig. 3. The vertical distance between platelets is d and the thickness of platelets is $2t$. w is the width of the platelet in the transverse direction. The platelets are in staggered arrangement, with the length of platelets given as $2L$ and length from the centre of one platelet to the beginning of next platelet is given as L_1. G is the shear modulus of the collagen matrix. The portion of the collagen matrix in between the platelets (horizontal) is considered to be an imaginary platelet with the same properties as that of the matrix. This is shown hatched in the figure. The real platelets are shown

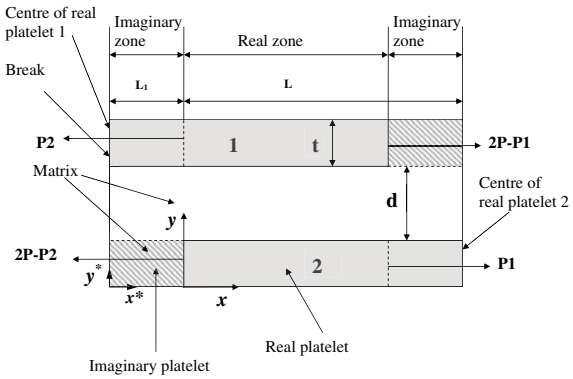

Figure 3: Idealised unit cell model

shaded. For the purpose of analysis, the unit cell is divided into the real zone (where both platelets are real) and imaginary zone (where at least one of the platelets is imaginary). x and y are the co-ordinates placed at the origin of the real zone and x^* and y^* are the co-ordinates placed at the origin of the imaginary zone. In all the equations a * denotes the imaginary zone. The shear stress is assumed to be constant in the matrix between the platelets. The platelet 1 is considered to be broken at its centre (see Fig. 3). The load is relieved by one platelet while it is taken up by the other platelet. The total load carried by the two platelets is $2P$. At the beginning of real zone of platelet 1, if the load carried is $P2$, then $2P-P2$ is the load carried by platelet 2 at the same section. At the end of real zone of platelet 2, if the load carried is $P1$, then the load carried by the platelet 1 is $2P-P1$.

The governing differential equations for real platelet 1 (real zone of platelet 1) is given by following equation (equation 1). This is derived based on the assumption that total load is shared by the two platelets.

$$\frac{d^2\sigma_{c1x}}{dx^2} - \frac{G}{td}\left(\frac{1}{E_1}+\frac{1}{E_2}\right)\sigma_{c1x} = -\frac{2PG}{wtE_2td} \qquad (1)$$

where E_1 and E_2 are the Young's modulus of platelet 1 and 2 respectively (both are equal in this case). The governing differential equation for the imaginary zone of platelet 1 is given by the following equation (equation 2).

$$\frac{d^2\sigma^*_{c1x}}{dx^2} - \frac{G}{td}\left(\frac{1}{E_1}+\frac{1}{E_3}\right)\sigma^*_{c1x} = -\frac{2PG}{wtE_3td} \quad (2)$$

where E_3 is the young's modulus of the matrix. Here σ_{c1x} and σ^*_{c1x} denote the axial stress in platelet 1 in the real and imaginary zones respectively.

The solution for the differential equations 1 and 2 are given by the following equations for the real zone and imaginary zone (equations 3 and 5). The subscript $_c$ denotes the variables and constants for the broken case.

$$\sigma_{c1x} = \frac{2P}{wtE_2\left(\frac{1}{E_1}+\frac{1}{E_2}\right)} + A_c cosh(\alpha x) + B_c sinh(\alpha x) \quad (3)$$

where α is given by expression 4

$$\alpha = \sqrt{\frac{G}{td}((1/E_1)+(1/E_2))} \quad (4)$$

$$\sigma^*_{c1x} = \frac{2P}{wtE_3\left(\frac{1}{E_1}+\frac{1}{E_3}\right)} + A^*_c cosh(\alpha^* x^*) + B^*_c sinh(\alpha^* x^*) \quad (5)$$

where α^* is given by the expression 6

$$\alpha^* = \sqrt{\frac{G}{td}((1/E_1)+(1/E_3))} \quad (6)$$

The formulation and solution obtained above are similar to that given by Kotha, Kotha, and Guzelsu (2000), for the case when there is no break in the platelet. The analysis described in this paper is for the case of a break at the center of platelet 1. The boundary conditions for the broken case, are different from that for the unbroken case and is given as follows.

1. Normal stress at break (centre of real platelet 1) is zero (see equation 7)

$$\sigma^*_{c1x}(x^* = 0) = 0 \quad (7)$$

2. Continuity of normal stress and shear stress at the end of imaginary zone and beginning of real zone of platelet 1. (see equations 8 and 9)

$$\sigma^*_{c1x}(x^* = L_1) = \sigma_{c1x}(x = 0) \quad (8)$$

$$\tau^*_{c1x}(x^* = L_1) = \tau_{c1x}(x = 0) \quad (9)$$

where τ_{c1x} and τ^*_{c1x} are the shear stresses in the real and imaginary zones of platelet 1.

3. The fourth boundary condition assumed is that normal stress at the end of real platelet 1 is the same for broken and unbroken case (refer equation 10).

$$\sigma_{c1x}(x = L - L_1) = \sigma_{1xend} \quad (10)$$

where σ_{1xend} is defined as the axial stress at the end of real platelet 1 for the case when there is no break at the centre of platelet 1 (Kotha, Kotha, and Guzelsu, 2000). The effect of break on the stress distribution in platelet 2 (and hence on platelet 1, since sum of axial stresses in the two platelets is a constant), will decrease as we move away from the break. The end of platelet 1 is sufficiently away from the break, which implies that the axial stress at this point for broken and unbroken cases would be equal, justifying our use of this assumption.

The application of the above boundary conditions yield the four constants A_c, B_c, A^*_c, B^*_c

$$A^*_c = -2P/wtE_3(1/E_1 + 1/E_3) \quad (11)$$

$$B_c{}^* = k3/k4 \quad (12)$$

where

$$k3 = \sigma_{1xend} - k_1 - [(\alpha^*/\alpha)A^*_c \sinh(\alpha^* L_1)\sinh(\alpha(L-L_1))] - [k_2 - k_1 + A^*_c \cosh(\alpha^* L_1)]\cosh(\alpha(L-L_1)) \quad (13)$$

$$k4 = \sinh(\alpha^* L_1)\cosh\alpha(L-L_1) + (\alpha^*/\alpha)\cosh(\alpha^* L_1)\sinh(\alpha(L-L_1)) \quad (14)$$

$$A_c = k_2 - k_1 + A_c^* \cosh(\alpha^* L_1) + B_c^* \sinh(\alpha^* L_1) \quad (15)$$

$$B_c = (\alpha^*/\alpha)[A_c^* \sinh(\alpha^* L_1) + B_c^* \cosh(\alpha^* L_1)] \quad (16)$$

where k_1 and k_2 are given by

$$k_1 = P/(wt) \quad (17)$$

$$k_2 = 2P/wtE_3(1/E_1 + 1/E_3) \quad (18)$$

The values of these constants are used in equations 3 and 5 to find the axial stress in real and imaginary zones of broken platelet 1. The axial stresses in the platelet 2 is found out invoking the assumption that the total load is carried by the two platelets together, as given by equation 19.

$$\sigma_{c1x} + \sigma_{c2x} = 2P/(wt) \quad (19)$$

The Matlab package (MathWorks, 2006) is used to calculate and plot the numerical results. In this work, parametric studies are conducted to find out the effect of change in overlapping ratio ($OR = L_1/t$), moduli ratio (E_1/E_3) and half the thickness of platelets (t).

2.2 Finite Element Analysis

Due to the simplified fiber and matrix representations, the shear lag analysis is computationally more efficient than detailed FE models. In spite of this simplification, shear lag analysis is able to capture many of the key features of deformation around broken fibers (Xia, Okabe, and Curtin, 2002). FE analysis for two cases of high and low OR are done using commercial finite element program ABAQUS (Hibbitt, Karlsson, and Sorensen, 2004) for comparison with shear lag analysis. Correlation of results from shear lag analysis with FEA for these two cases establishes the accuracy of the shear lag model used in this work as far as the axial stress distribution in platelet 2 is concerned. In view of this, studies are conducted employing shear lag theory for other geometrical values and the results obtained are expected to be accurate.

3 Results

Properties are selected for constituents of bone. Mineral platelets as well as collagen molecule are assumed to be linear elastic and isotropic. The material properties of collagen and mineral at the fine ultrastructure level is different from their macrolevel properties (Akkus, 2005). Hence, the numerical values of properties are selected so that they are close to the properties at that length scale. The Young's modulus of mineral platelets are taken to be 120 GPa and Poisson's ratio to be 0.27, which are similar to that obtained from powdered synthetic apatite and hence could be assumed to be values close to that of nano sized apatite crystal (Gilmore and Katz, 1982; Wagner and Weiner, 1992). The Young's modulus of collagen is taken to be 1.2 or 12 GPa , which are similar to values obtained for collagen molecule (Sasaki and Odajima, 1996). The Poisson's ratio of collagen is taken to be 0.35 (Doty, Robinson, and Schofield, 1976). These properties are similar to that used by other researchers (Wagner and Weiner, 1992; Kotha, Kotha, and Guzelsu, 2000; Akkus, 2005). In that sense, to a certain extent, the nanolevel characteristics are included in this model. Thus the arrangement is expected to take care of the effects which may be more likely at the nanolevel. However, the interface scale properties are not included in the analysis. Such effects that may depend on this may not be reflected in the analysis. The other constants are given the values, $L =$ 25nm, $t = 2.5/1.25$nm, $d = 1.25$nm, $w = 1$nm

Fig. 4– Fig. 6 show the axial stress distribution in platelet 2 along the axial direction from a section immediately below the break, which is at the centre of platelet 1, to the end of the unit cell. Graphs for three typical cases of overlapping ratios of 3.2, 1.4 and 0.04 ($L_1 = 8$, 3.5 and 0.1 nm respectively) are shown, which highlight the change in nature of stress distribution in platelet 2. The value of t is taken to be 2.5 nm and d as 1.25 nm. The mineral volume fraction, VF gets varied from about 60% to 80% upon variation of OR. The axial stresses are normalised with respect to the average remote stress acting on the edge of the unit cell. The distance from the centre of platelet 1 along the axial direction is normalised with respect to the length of unit cell. Fig. 7 and Fig. 8 show the results of the FE analysis conducted for two different overlapping ratios (3.2 and 0.04). For each

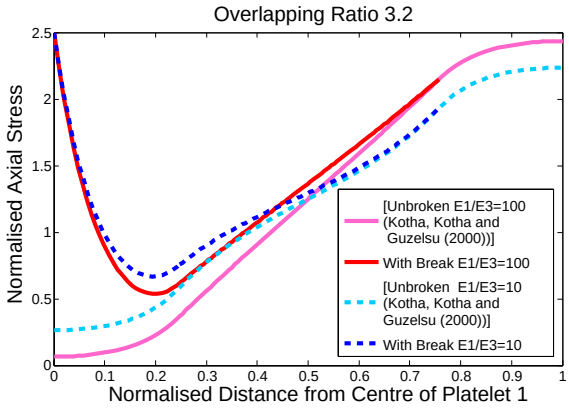

Figure 4: Axial stress distribution in platelet 2 using shear lag theory for an overlapping ratio of 3.2

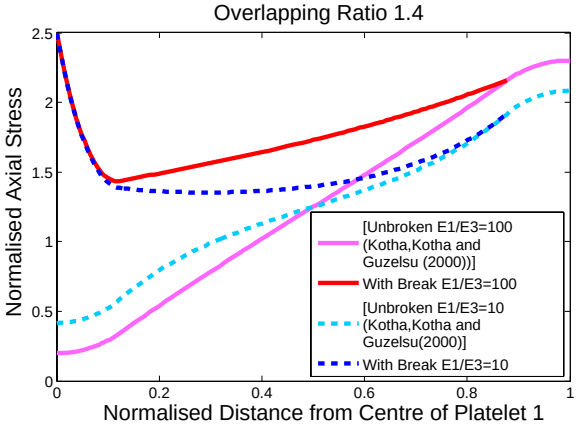

Figure 5: Axial stress distribution in platelet 2 using shear lag theory for an overlapping ratio of 1.4

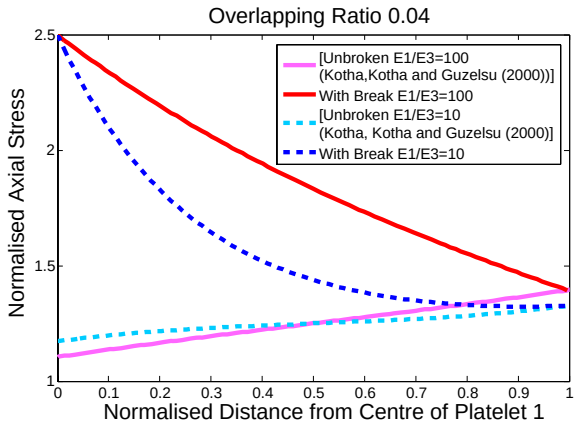

Figure 6: Axial stress distribution in platelet 2 using shear lag theory for an overlapping ratio of 0.04

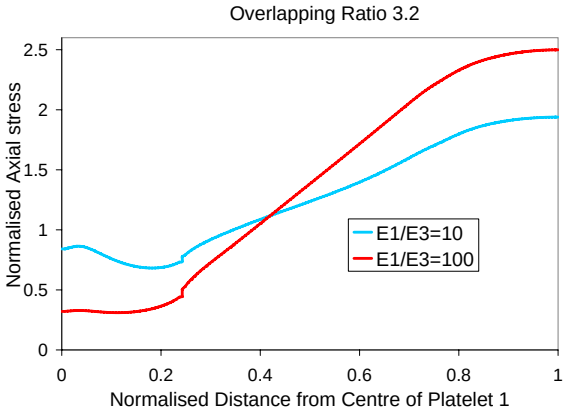

Figure 7: FE results of axial stress distribution in platelet 2 for an overlapping ratio of 3.2

case, graphs are drawn for two moduli ratios of 100 and 10.

Another study was conducted by using shear lag theory for a t value of 1.25 nm (d = 1.25 nm, L_1 = 8 nm , OR = 6.4, VF = 50.51%). This value of VF is near the mineral volume fraction in bone. Fig. 9 shows the axial stress distribution in platelet 2 along the x direction from a point immediately below the break, which is at the centre of platelet 1, for this case. The figure also shows the results of the parametric study conducted by changing the value of L_1 to 0.1 nm (OR = .08, VF= 66.40%), while keeping all the other dimensions constant. In all results employing shear lag theory, the stress distribution for unbroken case is also shown for comparison (Kotha, Kotha, and Guzelsu, 2000).

4 Discussion

The results show that there is a change in the the nature of stress distribution when overlapping ratio is varied (see Fig. 4−Fig. 6). As shown in Fig. 4, when overlapping ratio is high, there is a decrease in the axial stress followed by an increase. In the real zone of platelet 2 (real platelet 2), the stress increases toward the center

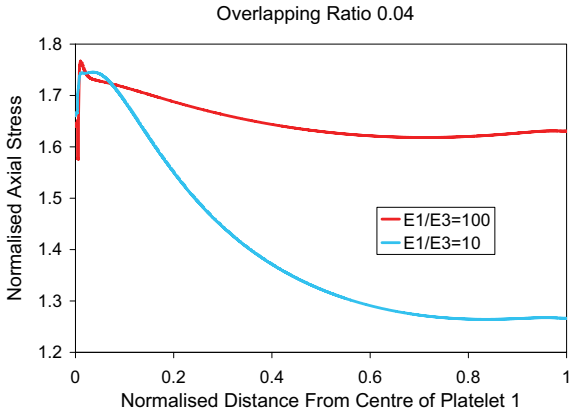

Figure 8: FE results of axial stress distribution in platelet 2 for an overlapping ratio of 0.04

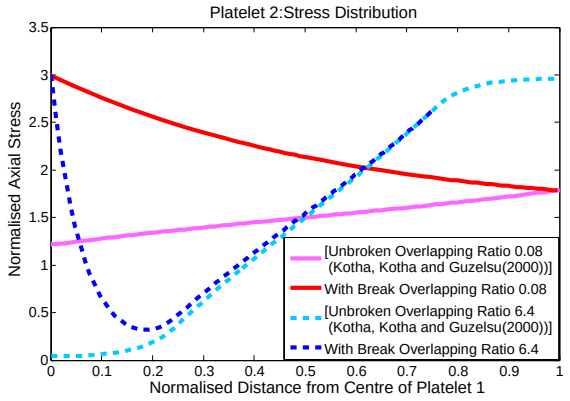

Figure 9: Stress distribution in platelet 2 employing shear lag theory for moduli ratio = 100: $t = d$ = 1.25 nm

of platelet 2. For very small overlapping ratio, the stress decreases from the point near the break to a point away from the break along the horizontal direction in platelet 2. This is the same nature of stress distribution that is observed in aligned platelets when one of them breaks (Wang and Qian, 2006). A transition stage between high and low overlapping ratios is shown in Fig. 5. This means that the nature of axial stress distribution in real platelet 2 depends on the overlapping ratio.

The shear lag results and FE results are in agreement as far as the axial stresses over the real platelet 2 is concerned. In the imaginary zone of platelet 2, the shear lag theory predicts much higher stresses than that obtained by FE analysis. This might be due to the assumption that sum of axial stresses in the two platelets is a constant. Hence when there is a break in platelet 1, all the stresses had to be carried by the imaginary zone of platelet 2, causing very high stresses here.

The Fig. 9 shows the stress distribution in platelet 2 for the case where t is equal to 1.25 nm. For large overlap, ($OR = 6.4$), the volume fraction of mineral in this case is 50.51%, which is close to volume fraction of mineral in bone. Also, mineral platelets in bone are arranged in a staggered manner, with a large overlap (Fratzl, Gupta, Paschalis, and Roschger, 2004). Here the thickness of platelets, $2t = 2.5$ nm and distance between platelets, $d = 1.25$ nm, which are very close to actual values of the nanostructure of bone (Rho, Kuhn-Spearing, and Zioupos, 1998). Hence this configuration could be assumed to be that which would represent structure of bone accurately at the nanolevel. The transition in the nature of stress distribution could be observed in this case also.

The analysis has been done for two different dimensions, yielding similar results about the influence of overlapping on the stress distribution in a platelet adjacent to a broken platelet. This suggests the importance of structural arrangement in two different areas, in design of composites as well as in the analysis bio-composites.

The mechanical properties of the material at lower length scales is different from that of the bulk material. This size effect has not been addressed in this paper directly. Also, the effect of interface scale properties has not been analysed. The effects that depend on interface scale properties may not get reflected in the analysis. However, since the properties that have been used are that at the scale of the fine ultrastructure, the results obtained are expected to be accurate to that extent. Further, the analysis has been done for two different moduli ratios, yielding similar results. This implies that the results obtained hold good even when there are some differences in the numerical values of properties.

The overlapping ratio may be expected to influ-

ence the fracture toughness of bio-composites. However, the formation and propagation of cracks depend on the constitutive behavior of materials, as well on other modes of failure like matrix cracking and debonding. Systematic consideration of all these factors is required to bring out the reasons for high fracture toughness of bio-composites.

In the present work, the shear stress in the matrix between platelets is assumed to be a constant. The volume fractions that we have considered are always greater than or equal to 50%. Hence the distance between the mineral platelets is smaller than that of the thickness of the platelets. This means that the constant shear stress assumption would provide sufficiently accurate results without making the analysis too complicated.

5 Conclusion

In this work, it is shown that the structural arrangement of mineral platelets influences the nature of stress distribution in the platelet adjacent to a broken platelet. The influence of overlapping ratio on the nature of stress distribution is elucidated. The way in which change in moduli ratio affect the stress distribution is also shown. However, together with determining the way in which overlapping affects fracture toughness of bio-composites, consideration of the effects of other parameters like constitutive behavior and other failure modes is important in a realistic understanding of the fracture toughness. Such an effort is ongoing, which would throw more light on the innate fracture resistant strategies of bio-composites.

Acknowledgement: The authors gratefully acknowledge the financial support under the QIP scheme of the AICTE, New Delhi. The authors also wish to thank Mr. Phani Kumar, for the help rendered with FE analysis and gratefully acknowledge Prof. Lakshmana Rao, for his valuable discussions and comments.

References

Akkus, O. (2005): Elastic deformation of mineralized collagen fibrils: An equivalent inclusion based composite model. *Journal of Biomechanical Engineering*, vol. 127, no. 3, pp. 383 – 390.

Doty, S.; Robinson, R. A.; Schofield, B. (1976): Morphology of bone and histochemical staining characteristics of bone cells. In Aurbach, G.(Ed): *Handbook of Physiology*. American Physiology Society, Washington, DC, USA.

Fratzl, P.; Gupta, H. S.; Paschalis, E. P.; Roschger, P. (2004): Structure and mechanical quality of the collagen-mineral nano-composite in bone. *Journal of Materials Chemistry*, vol. 14, no. 14, pp. 2115 – 2123.

Gilmore, R. S.; Katz, J. L. (1982): Elastic properties of apatites. *Journal of Materials Science*, vol. 17, no. 4, pp. 1131 – 41.

Goree, J. G.; Gross, R. S. (1980): Analysis of a unidirectional composite containing broken fibers and matrix damage. *Engineering Fracture Mechanics*, vol. 13, no. 3, pp. 563 – 578.

Hedgepeth, J. M. (1961): *Stress concentrations in filamentary structures*. NASA TND-882, Langley Research Center.

Hibbitt; Karlsson; Sorensen, I. (2004): ABAQUS standard user manual Version 6.5.

Ji, B.; Gao, H. (2004): Mechanical properties of nanostructure of biological materials. *Journal of the Mechanics and Physics of Solids*, vol. 52, no. 9, pp. 1963 – 1990.

Kotha, S. P.; Kotha, S.; Guzelsu, N. (2000): A shear-lag model to account for interaction effects between inclusions in composites reinforced with rectangular platelets. *Composites Science and Technology*, vol. 60, no. 11, pp. 2147 – 2158.

MathWorks, I. (2006): www.mathworks.com.

Menig, R.; Meyers, M. H.; Meyers, M. A.; Vecchio, K. S. (2000): Quasi-static and dynamic mechanical response of haliotis rufescens (abalone) shells. *Acta Materialia*, vol. 48, no. 9, pp. 2383 – 2398.

Muller-Karger, C. M.; Gonzalez, C.; Aliabadi, M. H.; Cerrolaza, M. (2001): Three dimensional bem and fem stress analysis of the human tibia under pathological conditions. *CMES: Computer Modeling in Engineering and Sciences*, vol. 2, no. 1, pp. 1 – 13.

Nalla, R. K.; Kruzic, J. J.; Kinney, J. H.; Balooch, M.; Ager III, J. W.; Ritchie, R. O. (2006): Role of microstructure in the aging-related deterioration of the toughness of human cortical bone. *Materials Science and Engineering C*, vol. 26, no. 8, pp. 1251 – 1260.

Nalla, R. K.; Kruzic, J. J.; Ritchie, R. O. (2004): On the origin of the toughness of mineralized tissue: microcracking or crack bridging? *Bone*, vol. 34, no. 5, pp. 790 –798.

Nukala, P. K. V. V.; Simunovic, S. (2005): A continuous damage random thresholds model for simulating the fracture behavior of nacre. *Biomaterials*, vol. 26, no. 30, pp. 6087 – 6098.

Reedy, E. D. J. (1984): Fiber stresses in a cracked monolayer: Comparison of shear-lag and 3-d finite element predictions. *Journal of Composite Materials*, vol. 18, no. 6, pp. 595 – 607.

Rho, J.-Y.; Kuhn-Spearing, L.; Zioupos, P. (1998): Mechanical properties and the hierarchical structure of bone. *Medical Engineering and Physics*, vol. 20, no. 2, pp. 92 – 102.

Sahar, N. D.; Hong, S.-I.; Kohn, D. H. (2005): Micro- and nano-structural analyses of damage in bone. *Micron*, vol. 36, no. 7-8, pp. 617 – 629.

Sasaki, N.; Odajima, S. (1996): Stress-strain curve and young's modulus of a collagen molecule as determined by the x-ray diffraction technique. *Journal of Biomechanics*, vol. 29, no. 5, pp. 655 – 658.

Schaffler, M. B.; Choi, K.; Milgrom, C. (1995): Aging and matrix microdamage accumulation in human compact bone. *Bone*, vol. 17, no. 6, pp. 521–525.

Vashishth, D.; Behiri, J. C.; Bonfield, W. (1997): Crack growth resistance in cortical bone: concept of microcrack toughening. *Journal of Biomechanics*, vol. 30, no. 8, pp. 763 – 769.

Wagner, H. D.; Weiner, S. (1992): On the relationship between the microstructure of bone and its mechanical stiffness. *Journal of Biomechanics*, vol. 25, no. 11, pp. 1311 – 1320.

Wang, X.; Qian, C. (2006): Prediction of microdamage formation using a mineral-collagen composite model of bone. *Journal of Biomechanics*, vol. 39, no. 4, pp. 595 – 602.

Xia, Z.; Okabe, T.; Curtin, W. A. (2002): Shear-lag versus finite element models for stress transfer in fiber-reinforced composites. *Composites Science and Technology*, vol. 62, no. 9, pp. 1141 – 1149.

Yeni, Y. N.; Fyhrie, D. P. (2002): Fatigue damage-fracture mechanics interaction in cortical bone. *Bone*, vol. 30, no. 3, pp. 509–514.

Zhang, P.; Klein, P.; Huang, Y.; Gao, H.; Wu, P. D. (2002): Numerical simulation of cohesive fracture by the virtual-internal-bond model. *CMES Computer Modeling in Engineering and Sciences*, vol. 3, no. 2, pp. 263 – 277.